



**HAL**  
open science

## CO<sub>2</sub> mass transfer and conversion to biomass in a horizontal gas–liquid photobioreactor

P. Valiorgue, H. Ben Hadid, M. El Hajem, L. Rimbaud, A. Muller-Feuga, J.Y.  
Champagne

► **To cite this version:**

P. Valiorgue, H. Ben Hadid, M. El Hajem, L. Rimbaud, A. Muller-Feuga, et al.. CO<sub>2</sub> mass transfer and conversion to biomass in a horizontal gas–liquid photobioreactor. *Chemical Engineering Research and Design*, 2014, 92 (10), pp.1891-1897. 10.1016/j.cherd.2014.02.021 . hal-04723535

**HAL Id: hal-04723535**

**<https://hal.science/hal-04723535v1>**

Submitted on 7 Oct 2024

**HAL** is a multi-disciplinary open access archive for the deposit and dissemination of scientific research documents, whether they are published or not. The documents may come from teaching and research institutions in France or abroad, or from public or private research centers.

L'archive ouverte pluridisciplinaire **HAL**, est destinée au dépôt et à la diffusion de documents scientifiques de niveau recherche, publiés ou non, émanant des établissements d'enseignement et de recherche français ou étrangers, des laboratoires publics ou privés.

## Accepted Manuscript

Title: CO<sub>2</sub> mass transfer and conversion to biomass in a horizontal gas-liquid photobioreactor

Author: P. Valiorgue H. Ben Hadid M. El Hajem L. Rimbaud  
A. Muller-Feuga J.Y. Champagne



PII: S0263-8762(14)00111-7  
DOI: <http://dx.doi.org/doi:10.1016/j.cherd.2014.02.021>  
Reference: CHERD 1509

To appear in:

Received date: 22-5-2013  
Revised date: 3-2-2014  
Accepted date: 17-2-2014

Please cite this article as: P. Valiorgue, H. Ben Hadid, M. El Hajem, L. Rimbaud, A. Muller-Feuga, J.Y. Champagne, CO<sub>2</sub> mass transfer and conversion to biomass in a horizontal gas-liquid photobioreactor, *Chemical Engineering Research and Design* (2014), <http://dx.doi.org/10.1016/j.cherd.2014.02.021>

This is a PDF file of an unedited manuscript that has been accepted for publication. As a service to our customers we are providing this early version of the manuscript. The manuscript will undergo copyediting, typesetting, and review of the resulting proof before it is published in its final form. Please note that during the production process errors may be discovered which could affect the content, and all legal disclaimers that apply to the journal pertain.

## Research Highlights

---

The CO<sub>2</sub> conversion to biomass efficiency is modelled.

The influence of gas stripping is shown to be not negligible.

Effects of design and operating parameters are investigated.

Accepted Manuscript

# CO<sub>2</sub> mass transfer and conversion to biomass in a horizontal gas-liquid photobioreactor

P. Valiorgue<sup>a,\*</sup>, H. Ben Hadid<sup>a</sup>, M. El Hajem<sup>a</sup>, L. Rimbaud<sup>b</sup>,  
A. Muller-Feuga<sup>b</sup>, J.Y. Champagne<sup>a</sup>

<sup>a</sup>*LMFA, UMR CNRS 5509, Université de Lyon, Ecole Centrale de Lyon,  
Université Lyon 1, INSA de Lyon, ECL, 20, avenue Albert Einstein - 69621  
Villeurbanne Cedex - tel: +33472436436, fax: +33472438718.*

<sup>b</sup>*Microphyt, 713, Route de Mudaison 34670 Baillargues - France,  
<http://www.microphyt.eu/>, Cell : +33 6 14 79 68 92*

---

## Abstract

This study deals with CO<sub>2</sub> mass transfers and biomass conversion in an industrial horizontal tubular photobioreactor. An analytical approach is used to determine an expression modeling the influence of CO<sub>2</sub> mass transfers on the overall biomass conversion efficiency for a given culture broth, heat and light conditions. Fluid mechanics and mass transfer are predicted with a classical two-phase flow approach [1] combined with a dissolution correlation developed and tested in the laboratory [2]. The influence of the stripping gas, removing the excess of oxygen in the liquid, on the conversion to biomass efficiency is shown to be not negligible. The expression is used to evaluate how the photobioreactor's design and process parameters can be tuned in order to improve biomass conversion efficiency. The biomass conversion efficiency evolution with the photobioreactor's length was found to behave asymptotically and it was explained by the relative orders of magnitude of gas dis-

solution and gas stripping. It has been shown that the gas flow rate for stripping and therefore the oxygen removal will be limited when further increasing the industrial photobioreactor's length for a given objective of CO<sub>2</sub> conversion to biomass efficiency.

*Key words:* mass transfer, gas-liquid, CO<sub>2</sub> biomass conversion, photobioreactor, microalgae.

---

## Nomenclature

### Greek symbols

$\eta$	Mass Transfer Efficiency (MTE),
$\nu$	Kinematic viscosity, [ $\frac{m^2}{s}$ ]
$\Phi$	Pipe diameter, [ $m$ ]
$\Phi_h$	Hydraulic diameter of the duct, [ $m$ ]
$\phi$	Molecular gas flux, [ $\frac{mol}{s \times m^2}$ ]
$\rho$	Density, [ $\frac{kg}{m^3}$ ]

### Latin symbols

$A$	Section area, [ $m^2$ ]
-----	-------------------------

---

\* Corresponding author.

*Email address:* pierre.valiorgue@gmail.com (P. Valiorgue).

$c$	Constant in the friction factor correlation
$C$	Carbon dioxide molar concentration, $[\frac{mol}{m^3}]$
$D$	Diffusion constant, $[\frac{m^2}{s}]$
$g$	Gravity, $[\frac{m}{s^2}]$
$h$	Height, $[m]$
$k$	Mass transfer coefficient, $[\frac{m}{s}]$ ,
$k_{La}$	Volumetric mass transfer coefficient, $[\frac{1}{s}]$ ,
$L_{tubes}$	Total tube length of the photobioreactor, $[m]$ ,
$M$	Molar mass, $[\frac{kg}{mol}]$
$m$	Carbon dioxide mass, $[kg]$
$p$	Pressure, $[Pa]$
$R$	Ideal gas constant, $[\frac{J}{mol.K}]$
$Re$	Reynolds number, $Re = \frac{U \cdot \Phi_h}{\nu}$
$S$	Perimeter, $[m]$
$Sc$	Schmidt number, $Sc = \frac{\nu}{D}$
$Sh$	Sherwood number, $Sh = \frac{k_L \cdot \Phi_h}{D}$
$T$	Temperature, $[K]$

$t$	Time, [s]
$U$	Mean velocity over the duct section area, [ $\frac{m}{s}$ ]
$v$	Exponent in equation (8), see Taitel in [1]
$w$	Exponent in equation (8), see Taitel in [1]
$x$	Coordinate in the downstream direction along the duct, [m]
$X$	Lockhart and Martinelli parameter.

### Subscripts and superscripts

$biomassconv$	CO <sub>2</sub> contained in the output dry microalgae,
$diss$	CO <sub>2</sub> dissolved,
$eq$	Equivalent height,
$G$	Gas,
$i$	Interface,
$injected$	CO <sub>2</sub> injected into the photobioreactor,
$L$	Liquid,
$undiss$	CO <sub>2</sub> undissolved and directly rejected to the atmosphere,
$prod$	Production of the microalgae mass harvested,
$residual$	CO <sub>2</sub> dissolved in the liquid and remaining dissolved,

$S$	Superficial, for single fluid flow,
$sat$	Saturation,
$stripped$	CO <sub>2</sub> driven to the atmosphere by the stripping air,
$\sim$	Dimensionless variable.

## 1 **1 Introduction**

2 Microalgae cultures have been recently regarded as a means to bioremediate  
3 industrial CO<sub>2</sub> waste. However, the efficiency of the conversion of the CO<sub>2</sub>  
4 into biomass has been seldom documented, and a significant part of the gas  
5 introduced in microalgae production systems is suspected of being released in  
6 the atmosphere. Improving the modelling of such biotechnological processes  
7 will help increasing the biomass conversion efficiency of industrial waste gas  
8 containing 10 to 20% of CO<sub>2</sub> [3–5]. High-density photoautotrophic microalgal  
9 growth in enclosed photobioreactors necessitates gas, light, momentum and  
10 heat exchanges [3,6]. Mass transfer modelling is a first step toward under-  
11 standing the coupled physics-biology in the photobioreactor and improving  
12 the CO<sub>2</sub> conversion to biomass.

13 This study deals with the experimental assessment and modelling of CO<sub>2</sub>  
14 biomass conversion in a horizontal co-current gas-liquid photobioreactor con-  
15 verting CO<sub>2</sub> into value-added microalgae. The windy, wavy and wiped tubular  
16 photobioreactor investigated has been designed for slow growing and fragile  
17 species with the ambition of improving accessibility to the huge biodiversity

18 of microalgae. For the purpose of reducing mechanical stress and avoiding cell  
19 wall disruption, the pump device is operated under low pressure and bubbling  
20 has been reduced by removing the direct airlift achieving mass transfer usu-  
21 ally placed in the culture loop [7,8]. Carbon dioxide and oxygen mass transfers  
22 are achieved through co-current circulation of gas and liquid within the pho-  
23 tobioreactor along with photosynthesis. Carbon is provided to the cells via  
24 punctual injections of gas that contains up to 10% of CO<sub>2</sub> and are monitored  
25 by a feedback loop maintaining a constant pH. Excess of oxygen inhibiting  
26 microalgae growth is removed from the culture broth by continuously injected  
27 stripping air [8,9].

28 A few mass transfer models and measurements applied to photobioreactors can  
29 be found in the literature of the two last decades. As highlighted in [10,11], CO<sub>2</sub>  
30 biomass conversion efficiency depends on CO<sub>2</sub> concentrations both in the air-  
31 CO<sub>2</sub> mixture injected in the photobioreactor and in the algal suspension [11].  
32 Therefore, mass transfer efficiencies (MTE) measurements should be reported  
33 for a given operating injected gas conditions as done in [11], for an outdoor  
34 culture of *Chlorella spirulina*. Very few data concerning the produced biomass  
35 and the injected mass of CO<sub>2</sub> are available in the literature as can be found  
36 in [11].

37 Mass transfer models of photobioreactors reported in the literature enable to  
38 determine overall mass transfer coefficients from correlations of the parame-  
39 ters of the process [12–15]. To our knowledge, there is no analytical study in  
40 the literature concerning CO<sub>2</sub> mass transfer and biomass conversion in a hor-  
41 izontal gas-liquid photobioreactor. Such an analytical study would determine  
42 where the CO<sub>2</sub> which has not been converted to biomass has been lost and  
43 how process parameters can be tuned in order to improve biomass conversion

44 efficiency for a given culture condition.

45 This paper is structured in three sections. In the first section, a CO<sub>2</sub> mass  
 46 balance over an horizontal photobioreactor will allow to express mass transfer  
 47 efficiencies as a function of operating parameters. Experimental measurements  
 48 will then be explained in the second section and finally, results will be pre-  
 49 sented and discussed.

## 50 **2 Mass transfer modeling**

### 51 *2.1 Conservation of mass*

52 As depicted on figure (1,a), the carbon dioxide mass injected in the photo-  
 53 bioreactor,  $m_{injected}$ , is partially dissolved into the liquid phase ( $m_{diss}$ ) and the  
 54 remaining part is directly rejected to the atmosphere, as written in equation  
 55 (1). The continuously injected air represented in figure (1,b) is also driving a  
 56 mass ( $m_{stripped}$ ) of carbon dioxide dissolved into the liquid to the atmosphere.  
 57 The carbon dioxide dissolved in the liquid phase will either be transformed into  
 58 biomass ( $m_{biomassconv}$ ) or remain as a dissolved form in the liquid ( $m_{residual}$ ),  
 59 as described by the mass balance written in equation (2).

$$m_{injected} = m_{undiss} + m_{diss} \quad (1)$$

$$m_{diss} = m_{stripped} + m_{residual} + m_{biomassconv} \quad (2)$$

60 Dividing equation (2) by the carbon dioxide mass injected, equation (3), the

61 photobioreactor's MTE is obtained. The photobioreactor's CO<sub>2</sub> conversion to  
 62 biomass MTE,  $\eta_{biomassconv}$ , is defined as the ratio of the carbon dioxide mass  
 63 contained in the output microalgae dry mass ( $m_{biomassconv}$ ) over the carbon  
 64 dioxide mass injected ( $m_{injected}$ ). Similarly,  $\eta_{diss}$ ,  $\eta_{stripped}$  and  $\eta_{residual}$  are de-  
 65 fined as the ratios of respectively  $m_{diss}$ ,  $m_{stripped}$  and  $m_{residual}$  over  $m_{injected}$ .

$$\eta_{biomassconv} = \eta_{diss} - \eta_{stripped} - \eta_{residual} \quad (3)$$

66 In the next sections, dissolution and stripping phases are modelled as functions  
 67 of process parameters .

## 68 2.2 Model for $\eta_{diss}$

69 As described in [7,8], the flow regime in the photobioreactor is mainly consti-  
 70 tuted of long slugs that are more or less wavy. From [2], a model for dissolution  
 71 efficiency ( $\eta_{diss}$ ) of an elongated gas bubble into a turbulent flow has been de-  
 72 veloped and is expressed in equation (4).

$$\eta_{diss} = 1 - e^{-k_L(Re) \times (C_{sat} - C) \times \frac{R \times T}{p \times h_G} \times t} \quad (4)$$

73 In this model, the interface is considered as a flat plane and the equivalent  
 74 bubble height  $h_G$ , is defined as the ratio of the cross section area occupied by  
 75 the gas,  $A_G$ , over the interfacial contact width  $S_i$ , see figure (2).

76 The contact time  $t$  between the bubble and the liquid is estimated from the gas  
 77 section area  $A_G$ , the photobioreactor's total length  $L_{tubes}$  and the gas flow rate  
 78  $Q_G$ , as expressed in equation (5). Replacing  $h_G$  and contact time into equation

79 (4) leads to the expression of  $\eta_{diss}$  as a function of operating parameters in  
80 equation (6).

$$t = \frac{A_G \times L_{tubes}}{Q_G} \quad (5)$$

$$\eta_{diss} = 1 - e^{-k_L(Re) \times (C_{sat} - C) \times \frac{R \times T}{p} \times \frac{S_i}{Q_G} \times L_{tubes}} \quad (6)$$

81 Estimations of the mass transfer coefficient and of the equivalent bubble height  
82 are required in order to evaluate  $\eta_{diss}$  from equation (6). The mass transfer  
83 coefficient  $k_L$ , has been evaluated using a correlation of the Sherwood number  
84  $Sh = \frac{k_L \cdot \Phi_h}{D}$ , the Schmidt number,  $Sc = \frac{\nu}{D}$ , and the Reynolds number,  $Re =$   
85  $\frac{U \cdot \Phi_h}{\nu}$ , proposed in Lamourelle [16] and expressed in equation (7) which has  
86 been tested successfully for an immobilised elongated bubble in [2].

$$Sh_L = 1.76 \times 10^{-5} \times Re^{1.506} \times Sc^{0.5} \quad (7)$$

87 In order to calculate the hydraulic diameter  $\Phi_h$ , the equivalent bubble height,  
88  $h_G$ , was estimated by solving the momentum balance equation (8) for hori-  
89 zontal stratified flow. In this dimensionless equation,  $X$  is the Lockhart and  
90 Martinelli's parameter defined in equation (9). The other dimensionless pa-  
91 rameters in equation (8) are explicitly defined in [17] as a function of the  
92 dimensionless liquid height,  $\tilde{h}_L$ .

$$X^2 \left[ (\tilde{U}_L \tilde{\Phi}_L)^{-v} \tilde{U}_L^2 \frac{\tilde{S}_L}{\tilde{A}_L} \right] - \left[ (\tilde{U}_G \tilde{\Phi}_G)^{-w} \tilde{U}_G^2 \left( \frac{\tilde{S}_G}{\tilde{A}_G} + \frac{\tilde{S}_i}{\tilde{A}_L} + \frac{\tilde{S}_i}{\tilde{A}_G} \right) \right] = 0 \quad (8)$$

$$X^2 = \frac{\left| \left( \frac{dp}{dx} \right)_{S,L} \right|}{\left| \left( \frac{dp}{dx} \right)_{S,G} \right|} = \frac{\frac{4c_L}{\Phi} \left( \frac{U_{S,L}\Phi}{\nu_L} \right)^{-v} \frac{\rho_L(U_{S,L})^2}{2}}{\frac{4c_G}{\Phi} \left( \frac{U_{S,G}\Phi}{\nu_G} \right)^{-w} \frac{\rho_G(U_{S,G})^2}{2}} \quad (9)$$

93 A relationship between liquid flow rate, gas flow rate and liquid height can be  
 94 expressed replacing equation (9) into equation (8). The obtained equation is  
 95 solved for  $\tilde{h}_L$  using dichotomy knowing the gas and liquid velocities for the  
 96 guessed liquid height.

97 A Scilab algorithm calculates the mass transfer coefficient and the mass trans-  
 98 fer efficiency for each rectilinear section of the photobioreactor using respec-  
 99 tively Lamourelle's correlation (7) and equation (6).

### 100 2.3 Model for $\eta_{stripped}$

101 As the stripping air is injected continuously, the interface is distributed along  
 102 the entire length of the photobioreactor. The interface for the gas-liquid flow  
 103 is approximated to  $S_i \times L_{tubes}$ . The interface width  $S_i$  is considered as a con-  
 104 stant along the photobioreactor's length since the mass transferred is small  
 105 compared to the mass injected.

106 As noted by Boettcher in [18], the molecular gas flux through a gas-liquid  
 107 interface can be expressed as a function of the local molar concentration  $C$   
 108 and the molar concentration at saturation of the stripping gas  $C_{sat\ stripped}$  by  
 109 equation (10).

$$\frac{dn_{stripped}}{dt} = -(S_i \times L_{tubes}) \times \phi = -k_L \times (S_i \times L_{tubes}) \times (C_{sat\ stripped} - C) \quad (10)$$

110 Integrating equation (10) with respect to time, the stripping MTE can be  
 111 expressed as in equation (11).

$$\eta_{stripped} = -k_L \times (S_i \times L_{tubes}) \times (C_{sat\ stripped} - C) \times M_{CO_2} \times \frac{t_{prod}}{m_{injected}} \quad (11)$$

112 In equation (11), the coupled effects of cell density, light, momentum or tem-  
 113 perature influencing the culture growth are affecting the stripping phase and  
 114 therefore the CO<sub>2</sub> conversion to biomass process. They are implicitly taken  
 115 into account through  $t_{prod}$ , the production time.

116 In order to evaluate mass transfer efficiencies, mass transfer measurements  
 117 in an industrial photobioreactor have been realised and their acquisition is  
 118 described in the following section.

### 119 3 Measurements of Mass Transfer Efficiencies

120 During data acquisitions, the microalgae specie cultivated in the photobio-  
 121 actor is chlorophyte *Neochloris oleoabundans*. The aim of the measurements in  
 122 the photobioreactor is to determine the orders of magnitudes for dissolution,  
 123 stripping and photobioreactor's MTEs.

124 3.1 Measurement of  $\eta_{diss}$

125 A Gastec CO<sub>2</sub> dosage kit has been used for the measurements. These kits  
126 are given for carbon dioxide concentrations from 0.5 to 20 % of the volume.  
127 During data acquisition, injection flow rates of air and CO<sub>2</sub> have been set  
128 with an injected gas containing up to 10% of CO<sub>2</sub>. Measurements of CO<sub>2</sub>  
129 concentration at the injection point and the exit of the photobioreactor show  
130 a dissolution MTE,  $\eta_{diss}$ , of 72%. The coefficient of variation of 5% given  
131 for this probe is considered as the relative error for each measurement. The  
132 relative error on  $\eta_{diss}$  is then of 10%.

133 3.2 Measurement of  $\eta_{biomassconv}$

134 From its definition,  $\eta_{biomassconv}$  evaluation requires the measurement of the  
135 harvested microalgae's dry mass and of the consumed mass of CO<sub>2</sub> to produce  
136 it, considering that  $\eta_{residual}$  is considered to be negligible. The residual mass  
137 of dissolved CO<sub>2</sub> in the culture broth photobioreactor has been measured with  
138 a metler toledo inPro 5000 and is evaluated to be less than 20 mg/L.

139 During the photobioreactor's development phase, food grade carbon dioxide  
140 gas bottles of 37.4 kg were used to feed microalgae. The injected mass of CO<sub>2</sub>  
141 have been estimated from the gas bottles' weight.

142 From June 16<sup>th</sup> to July 7<sup>th</sup>, 18.54 kilograms of dry biomass were harvested. It  
143 should be noted that, from the photosynthesis' stoichiometry for *Neochloris*  
144 *oleoabundans* given in [19], 1.88 grams of CO<sub>2</sub> are converted to biomass when  
145 1 gram of dry microalgae is produced. This coefficient is then applied in order

146 to find the equivalent gas mass of CO<sub>2</sub> contained into the produced mass of  
147 microalgae.

148 As can be seen in figure (3), microalgae concentration evolution with time  
149 was maintained in a small range over the 22 days harvesting period. The final  
150 cell density was measured around  $1.6 \times 10^8$  cells per millilitre, higher than  
151 the starting cell density around  $1 \times 10^8$  cells per millilitre. Given that on  
152 average 1.7 g of dry biomass were harvested from a litre of culture broth for  
153 an average cell density of  $1.3 \times 10^8$  cells per millilitre, the equivalent of 3.69  
154 kg dry biomass have been produced without being harvested. Using Pruvost  
155 [19], 34.85 kg of CO<sub>2</sub> were converted into the harvested dry biomass which has  
156 been produced using 105.4 kg of CO<sub>2</sub> gas. The minimum biomass conversion  
157 efficiency is then estimated to 33% considering only the carbon fraction in  
158 the harvested biomass. Considering that 3.69 kg of dry biomass that have  
159 been estimated to remain in the photobioreactor without being harvested, the  
160 maximum biomass conversion efficiency is estimated to 40%.

### 161 3.3 Evaluation of $\eta_{stripped}$

162  $\eta_{stripped}$  is evaluated from equation (3). The error is the sum of errors on  $\eta_{diss}$   
163 and  $\eta_{biomassconv}$ . For the considered culture conditions, orders of magnitude  
164 of  $\eta_{stripped}$  and  $\eta_{biomassconv}$  are similar. Considering that from equation (11),  
165  $\eta_{stripped}$  is proportional to production time,  $t_{prod}$ , if the time of production  
166 is reduced, the photobioreactor's MTE will increase by the same proportion.  
167 As a consequence, research efforts on optimum light, momentum and heat  
168 conditions for microalgae's growth rate will have a strong impact on the global  
169 photobioreactor's CO<sub>2</sub> conversion to biomass efficiency.

170 **4 Results and discussion**

171 *4.1 Dissolution model*

172 The dissolution model presented in section 2.2 is plotted against the dissolu-  
 173 tion measurement on figure (4). Asterisk and plus marks in the figure represent  
 174 the abscissa at the end of a linear section of the photobioreactor along which  
 175 the liquid height, CO<sub>2</sub> concentration, pressure and mass flow rates are consid-  
 176 ered as constants. For the considered conditions, carbon dioxide is dissolved  
 177 regularly along the photobioreactor. A good agreement was found between  
 178 dissolution measurements on the photobioreactor and the dissolution model.  
 179 The order of magnitude of the influence of the injected gas carbon dioxide  
 180 concentration can also be evaluated from figure (4).

181 Another result from the dissolution model concerns optimum flow conditions  
 182 for dissolution. As expressed in equation (6), for a fixed photobioreactor's  
 183 length, dissolution is improved when the ratio  $\frac{k_L(Re) \times S_i}{Q_G}$  is as large as possible.  
 184 This ratio is a function of three variables  $Q_G$ ,  $Q_L$  and  $h_L$  that are related by the  
 185 momentum balance equation (8). For industrial parameters  $5 < Q_G \left[ \frac{Nl}{min} \right] <$   
 186  $100$  and  $20 < Q_L \left[ \frac{l}{min} \right] < 450$ ,  $\tilde{h}_L$  and  $S_i$  can be considered as constants  
 187 since the standard deviations are evaluated as respectively 6% and 8.5% of  
 188 the averaged values, for the considered flow rates. As a consequence, effects of  
 189  $Q_L$  and  $Q_G$  on  $\frac{k_L(Re) \times S_i}{Q_G}$  are decoupled. Practically, as can be seen on figure  
 190 (5) for the range of considered flow rates, dissolution will be improved by  
 191 increasing the liquid flow rate and therefore turbulence or by decreasing the  
 192 gas flow rates and thus enhancing contact time, as long as the flow rates are  
 193 compatible with culture conditions.

194 *4.2 Influence of dissolution and stripping on the photobioreactor's MTE and*  
 195 *optimum length*

196 Combining equations (3), (6) and (11), an expression of  $\eta_{biomassconv}$  as a func-  
 197 tion of the photobioreactor's length,  $L_{tubes}$ , is obtained. In order to assess the  
 198 interest of scaling, it is possible to derive an semi-empirical relation for the  
 199 optimum length of the photobioreactor considering an equivalent constant con-  
 200 centration gradient along the photobioreactor as expressed in equation (12).

$$L_{opti} = \frac{L_{tubes}}{1 - \eta_{diss}(L_{tubes})} \times \ln \left( \frac{\eta_{diss}(L_{tubes}) - \eta_{biomassconv}(L_{tubes})}{\ln \left( \frac{1}{1 - \eta_{diss}(L_{tubes})} \right)} \right) \quad (12)$$

201 For the considered conditions, the optimum length and relative influence of  
 202 dissolution and stripping on scaling for the photobioreactor's MTE are plot-  
 203 ted in figure (6). It appears that the photobioreactor's length is close to the  
 204 optimum length for carbon dioxide CO<sub>2</sub> conversion to biomass efficiency for  
 205 the operated conditions.

206 **5 Conclusion**

207 An analysis of mass transfer in a horizontal photobioreactor based on a mass  
 208 balance has been presented. The influence of the CO<sub>2</sub> dissolved in the liquid  
 209 and remaining dissolved have been shown to be negligible compared to the  
 210 injected CO<sub>2</sub> mass during the measurements. Under such conditions, strip-  
 211 ping effects have been determined using dissolution and conversion to biomass  
 212 measurements. They were found to be not negligible. A good agreement was

213 found between dissolution measurements and results predicted by the theo-  
214 retical prediction from the dissolution model for elongated bubbles adapted  
215 for two phase flow. The influence of injected  $\text{CO}_2$  concentration and flow rates  
216 on the dissolution efficiency as predicted by the dissolution model have been  
217 emphasized. A numerical investigation of the dissolution model highlighted  
218 the effects of gas and liquid flow rates on the dissolution efficiency. Effects of  
219 dissolution and stripping on the asymptotic behaviour of biomass conversion  
220 efficiency evolution with the photobioreactor's length for given culture con-  
221 ditions were identified. It is expected that stripping will have to be reduced  
222 when further increasing the photobioreactor's length for a given  $\text{CO}_2$  conver-  
223 sion to biomass efficiency objective. Research efforts on optimum growth rate  
224 conditions and growth rate with oxygen will contribute to diminish the lim-  
225 iting effects of stripping and improve the global photobioreactor's conversion  
226 to biomass prediction and efficiency.

227 **References**

- 228 [1] Y. Taitel, A. E. Dukler, A model for predicting flow regime transitions in  
229 horizontal and near horizontal gas-liquid flow, *AIChE Journal* 22 (1) (1976)  
230 47–55.
- 231 [2] P. Valiorgue, M. Hajem, A. Vassilev, V. Botton, H. Hadid, Elongated gas bubble  
232 dissolution under a turbulent liquid flow, *Chemical Engineering and Processing:  
233 Process Intensification* (2011).
- 234 [3] L. Cheng, L. Zhang, H. Chen, C. Gao, Carbon dioxide removal from  
235 air by microalgae cultured in a membrane-photobioreactor, *Separation and  
236 Purification Technology* 50 (3) (2006) 324–329.
- 237 [4] D. Ayhan, Biodiesel from oilgae, biofixation of carbon dioxide by microalgae:  
238 A solution to pollution problems, *Applied Energy* 88 (10) (2011) 3541–3547.
- 239 [5] K. G. Zeiler, D. A. Heacox, S. T. Toon, K. L. Kadam, L. M. Brown, The use of  
240 microalgae for assimilation and utilization of carbon dioxide from fossil fuel-fired  
241 power plant flue gas, *Energy Conversion and Management* 36 (6-9) 707–712.
- 242 [6] R. K. Mandalam, B. Palsson, Elemental balancing of biomass and medium  
243 composition enhances growth capacity in high-density *Chlorella vulgaris*  
244 cultures, *Biotechnology and Bioengineering* 59 (5) (1998) 605–611.
- 245 [7] A. Muller-Feuga, M. Lemar, E. Vermel, R. Pradelles, L. Rimbaud, P. Valiorgue,  
246 M. El Hajem, J. Champagne, Appraisal of a Horizontal Two-phase Flow  
247 Photobioreactor for Industrial Production of Delicate Microalgae Species,  
248 *Journal of Applied Phycology* 24 (3) (2012) 349–355
- 249 [8] A. Muller-Feuga, M. Lemar, E. Vermel, R. Pradelles, L. Rimbaud, P. Valiorgue,  
250 M. El Hajem, J. Champagne, Design and assessment of an industrial windy,

- 251 wavy and wiped tubular photobioreactor, in: 4th congress of International  
252 Society for Applied Phycology, Halifax, Canada, 2011.
- 253 [9] T. Ogawa, T. Fujii, S. Aiba, Effect of oxygen on the growth (yield) of *Chlorella*  
254 *vulgaris*, *Archives of Microbiology* 127 (1) (1980) 25–31.
- 255 [10] T. M. Sobczuk, F. G. Camacho, F. C. Rubio, F. G. A. Fernández, E. M. Grima,  
256 Carbon dioxide uptake efficiency by outdoor microalgal cultures in tubular  
257 airlift photobioreactors, *Biotechnology and Bioengineering* 67 (4) (2000) 465–  
258 475.
- 259 [11] J. Doucha, F. Straka, K. Lívanský, Utilization of flue gas for cultivation of  
260 microalgae (*Chlorella* sp.) in an outdoor open thin-layer photobioreactor, *Journal*  
261 *of Applied Phycology* 17 (5) (2005) 403–12.
- 262 [12] D. Baquerisse, Modelling of a continuous pilot photobioreactor for microalgae  
263 production, *Journal of Biotechnology* 70 (1-3) (1999) 335–342.
- 264 [13] K. Loubiere, J. Pruvost, F. Aloui, J. Legrand, Investigations in an external-loop  
265 airlift photobioreactor with annular light chambers and swirling flow, *Chemical*  
266 *Engineering Research and Design* 89 (2) (2011) 164–171.
- 267 [14] R. Reyna-Velarde, E. Cristiani-Urbina, D. J. Hernández-Melchor, F. Thalasso,  
268 R. O. Cañizares-Villanueva, Hydrodynamic and mass transfer characterization  
269 of a flat-panel airlift photobioreactor with high light path, *Chemical Engineering*  
270 *and Processing: Process Intensification* 49 (1) (2010) 97–103.
- 271 [15] L. Fan, Y. Zhang, L. Zhang, H. Chen, Evaluation of a membrane-sparged helical  
272 tubular photobioreactor for carbon dioxide biofixation by *Chlorella vulgaris*,  
273 *Journal of Membrane Science* 325 (1) (2008) 336–345.
- 274 [16] A. P. Lamourelle, O. C. Sandall, Gas absorption into a turbulent liquid,  
275 *Chemical Engineering Science* 27 (5) (1972) 1035–1043.

- 276 [17] A. E. Dukler, Y. Taitel, Flow pattern transitions in gas-liquid systems:  
 277 measurement and modeling 2 (1-4) (1986) 1–94.
- 278 [18] E. Boettcher, J. Fineberg, D. Lathrop, Turbulence and wave breaking effects  
 279 on air-water gas exchange, Physical Review Letters 85 (9) (2000) 2030–2033.
- 280 [19] J. Pruvost, G. Van Vooren, G. Cogne, J. Legrand, Investigation of biomass and  
 281 lipids production with neochloris oleoabundans in photobioreactor, Bioresource  
 282 Technology 100 (23) (2009) 5988–5995.

### 283 Captions for tables and figures

Fig. 1. Diagram of the carbon dioxide punctual dissolution phase (a) and continuous air stripping phase (b).

Fig. 2. Summary of the notations used in this article are defined to be congruent to Taitel [1].

Fig. 3. Cell density evolution with time and details for the measurement period.

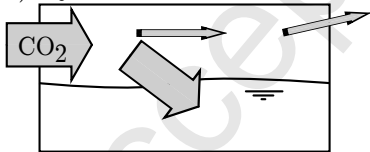
Fig. 4. Dissolution MTE,  $\eta_{diss}$ , as a function of the total tube length of the photobioreactor,  $L_{tubes}$ , and injected gas concentration as predicted by the one-dimensional model presented in section 2.2. The liquid and gas flow rates used,  $Q_L$  and  $Q_G$ , were corresponding to the experimental measurement operating flow rates on Microphyt's photobioreactor, respectively 130 l/min and 35 N.l/min.

Fig. 5. The ratio  $\frac{k_L(Re) \times S_i}{Q_G}$  is a function of  $Q_L$  and  $Q_G$ . Flow rates maximising this ratio are the optimum flow rates for dissolution.

Fig. 6. Measurements and extrapolation of the evolution of  $\eta_{biomassconv}$ ,  $\eta_{diss}$  and  $\eta_{stripped}$  as a function of the total tube length of the photobioreactor,  $L_{tubes}$ , for carbon dioxide concentration in the injected gas up to 10% and non-optimised flow rates.

**Figure 01**

a) Injection



b) Stripping

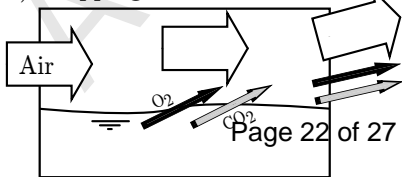
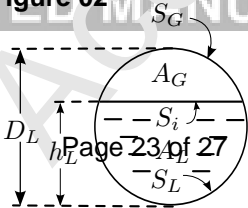


Figure 02



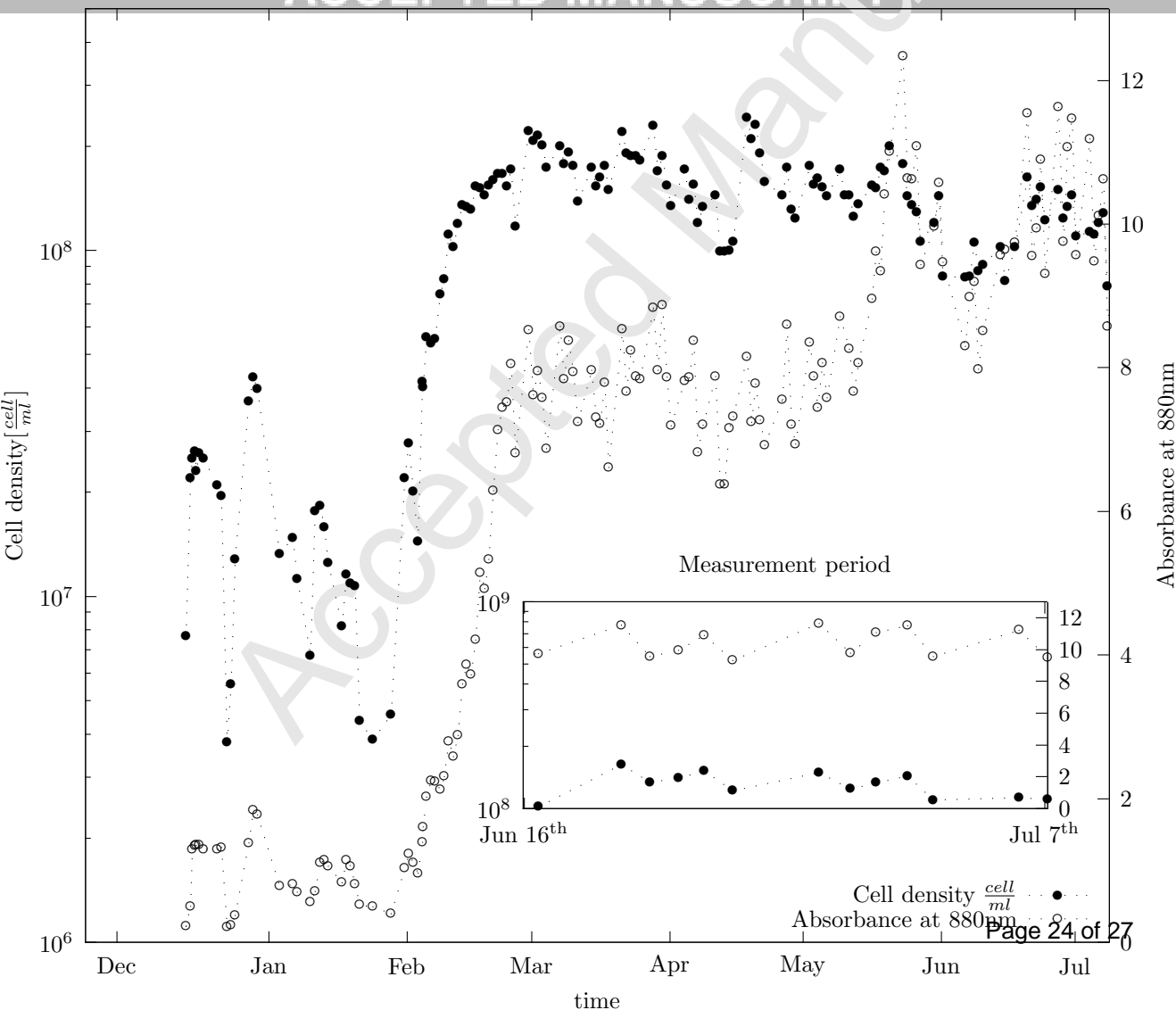


Figure 04

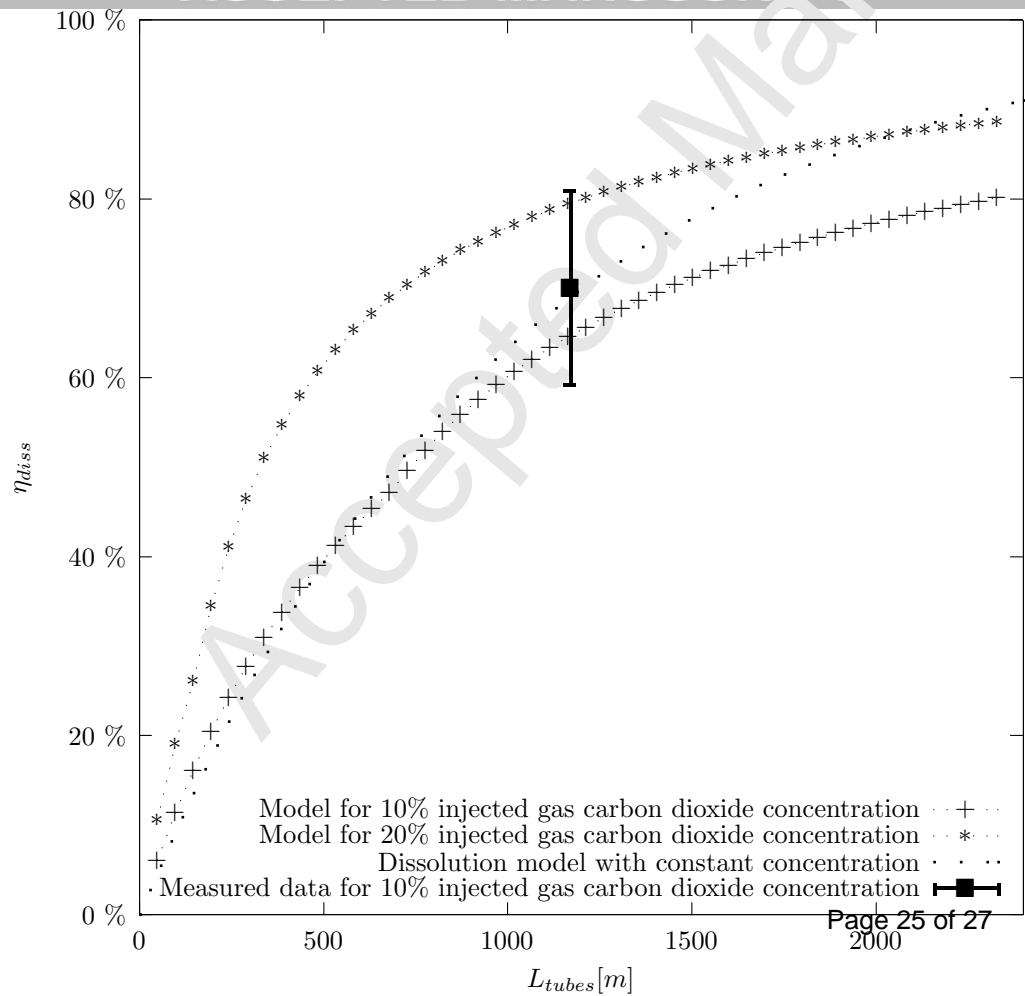
ACCEPTED MANUSCRIPT  
Influence of concentration and photobioreactor's length on  $\eta_{diss}$ 

Figure 05

ACCEPTED MANUSCRIPT

